Journal of Inclusion Phenomena and Molecular Recognition in Chemistry **11**: 247–256, 1991.

Crystal Structures of Bile Salts: Sodium Taurocholate

ANNA RITA CAMPANELLI, SOFIA CANDELORO DE SANCTIS, ANGELO ANTONIO D'ARCHIVIO, and EDOARDO GIGLIO*
Dipartimento di Chimica, Università di Roma 'La Sapienza', P.le A. Moro 5, 00185 Rome, Italy

LUCIO SCARAMUZZA
Istituto di Teoria e Struttura Elettronica e Comportamento Spettrochimico dei Composti di Coordinazione del C.N.R., Area della Ricerca, CP 10, 00016 Monterotondo Stazione, Rome, Italy

(Received: 21 February 1991; in final form: 13 June 1991)

Abstract. Crystals of sodium taurocholate ($NaC_{26}H_{44}NO_7S \cdot 2.5\,H_2O$) belonging to the triclinic space group $P1$ have unit cell parameters $a = 12.731$ (2), $b = 16.104$ (2), $c = 7.628$ (1) Å, $\alpha = 83.40$ (1), $\beta = 101.20$ (1), $\gamma = 105.35$ (1)°, and two molecules in the asymmetric unit. The refinement, carried out on 4424 observed reflections, gave $R = 0.059$ and $R_w = 0.066$. The packing is characterized by bilayers, formed by antiparallel monolayers and with nonpolar outermost surfaces, held together by van der Waals interactions. Inside the bilayers there are channels, lined with polar groups, and filled by sodium ions and water molecules. A structural unit has been identified that could provide a reasonable model for the micellar aggregates of this bile salt.

Key words. Sodium taurocholate, X-ray crystal structure, micellar aggregate model.

Supplementary Data relevant to this article have been deposited with the British Library under the reference number SUP 82125 (38 pages).

1. Introduction

It has previously been shown that a helical model suitable for the representation of the micellar aggregates of sodium and rubidium deoxycholate (NaDC and RbDC, respectively) in aqueous solutions can be inferred from the structural units observed in the crystals of these compounds [1–4, and references therein]. Small-angle X-ray scattering [2], extended X-ray absorption fine structure [3], electron spin resonance [2], circular dichroism [5, 6] and nuclear magnetic resonance [1, 7, 8] measurements performed on aqueous micellar solutions, some of which contained probe molecules such as hydrocarbons [1, 5], bilirubin-IXα [6], a spin-labelled cholestane which mimics cholesterol [7], and acridine orange [8], confirmed the proposed helical model. In order to obtain possible models for the micellar structures of some bile salts, which are important from a biological point of view [9, and references therein], the crystal structures of sodium glycodeoxycholate (NaGDC) [6], taurodeoxycholate (NaTDC) [10] and glycocholate (NaGC) [11] were solved, in addition to that of RbDC [12], and, again, helical models were found. This paper deals with the crystal structure of a triclinic phase of sodium taurocholate (NaTC), one of the most important and carefully studied conjugated bile salts in humans.

*Author for correspondence.

2. Experimental

2.1. CRYSTAL DATA

Single crystals of NaTC containing water were grown by diffusion of acetone vapour into an aqueous solution of the bile salt. After about one week, prismatic colourless crystals, m.p. 451–453 K, precipitated. They corresponded to one of the three crystalline phases, obtained under various conditions, previously reported in the literature [13].

The cell constants, refined by least-squares from 25 centered reflections together with the orientation matrix, are: $a = 12.731$ (2), $b = 16.104$ (2), $c = 7.628$ (1) Å, $\alpha = 83.40$ (1), $\beta = 101.20$ (1), $\gamma = 105.35$ (1)°, $V = 1476.0$ (4) Å^3. The space group is $P1$ and the asymmetric unit is 2 NaTC + 5 H_2O molecules. The calculated crystal density (1.31 g cm^{-3}) agrees with the experimental one (1.31 g cm^{-3}) measured by flotation using a chloroform–chlorobenzene mixture, the density of which was determined by means of a DMA 02C densimeter.

A single crystal of approximate dimensions $0.2 \times 0.3 \times 0.7$ mm was mounted on a Nonius CAD4 diffractometer using graphite-monochromated MoK_α radiation ($\lambda = 0.70926$ Å). A total of 4424 independent reflections with $I > 3\sigma(I)$ were collected at room temperature using the ω–2θ scan mode in the range $4 \leqslant 2\theta \leqslant 50°$, with $\omega = (0.7 + 0.35 \tan\theta)°$. The scan speed varied from 5.5 to 0.6 deg min^{-1} as a function of reflection intensity. Three standard reflections were measured every 160 min to monitor intensity variations; negligible decay was observed. The intensities were corrected for Lorentz and polarization effects but not for absorption ($\mu = 1.82$ cm^{-1}).

2.2. STRUCTURE DETERMINATION AND REFINEMENT

The structure was solved using direct methods (MULTAN 88) [14]. An E-map showed most of the non-H atoms. The remaining atoms were located by means of successive Fourier syntheses and structure factor calculations. The refinement was carried out with the program CRYSTALS [15] using a block full-matrix least-squares method. Two blocks were formed, the first with the parameters of one NaTC anion, and the second with those of the other NaTC anion, the two sodium ions, and the oxygen atoms of five water molecules. Atomic scattering factors, including real and imaginary dispersion corrections for sulphur atoms and sodium ions, were taken from the *International Tables for X-ray Crystallography* [16]. All non-H atoms were refined anisotropically, except N(64), C(65), C(66), O(69), and O(5), which appeared in the Fourier syntheses with electron densities lower than those of similar atoms, and during the refinement exhibited some abnormally high anisotropic temperature factors. Hydrogen atoms were generated at the expected positions, except for those of water molecules and hydroxyl groups, which were not taken into account in any calculation. Hydrogen atoms' coordinates and isotropic thermal parameters were calculated at each cycle of refinement from those of the parent atoms. The function minimized was $\Sigma\, w(|F_o| - |F_c|)^2$ with $w = (\sin\theta/\lambda)^2$. Some other weighting schemes gave slightly worse results. Final agreement factors were $R = 0.059$ and $R_w = 0.066$.

The atomic positional and equivalent isotropic thermal parameters are reported in Table I, in accordance with the atom labelling of Figure 1, where bond lengths

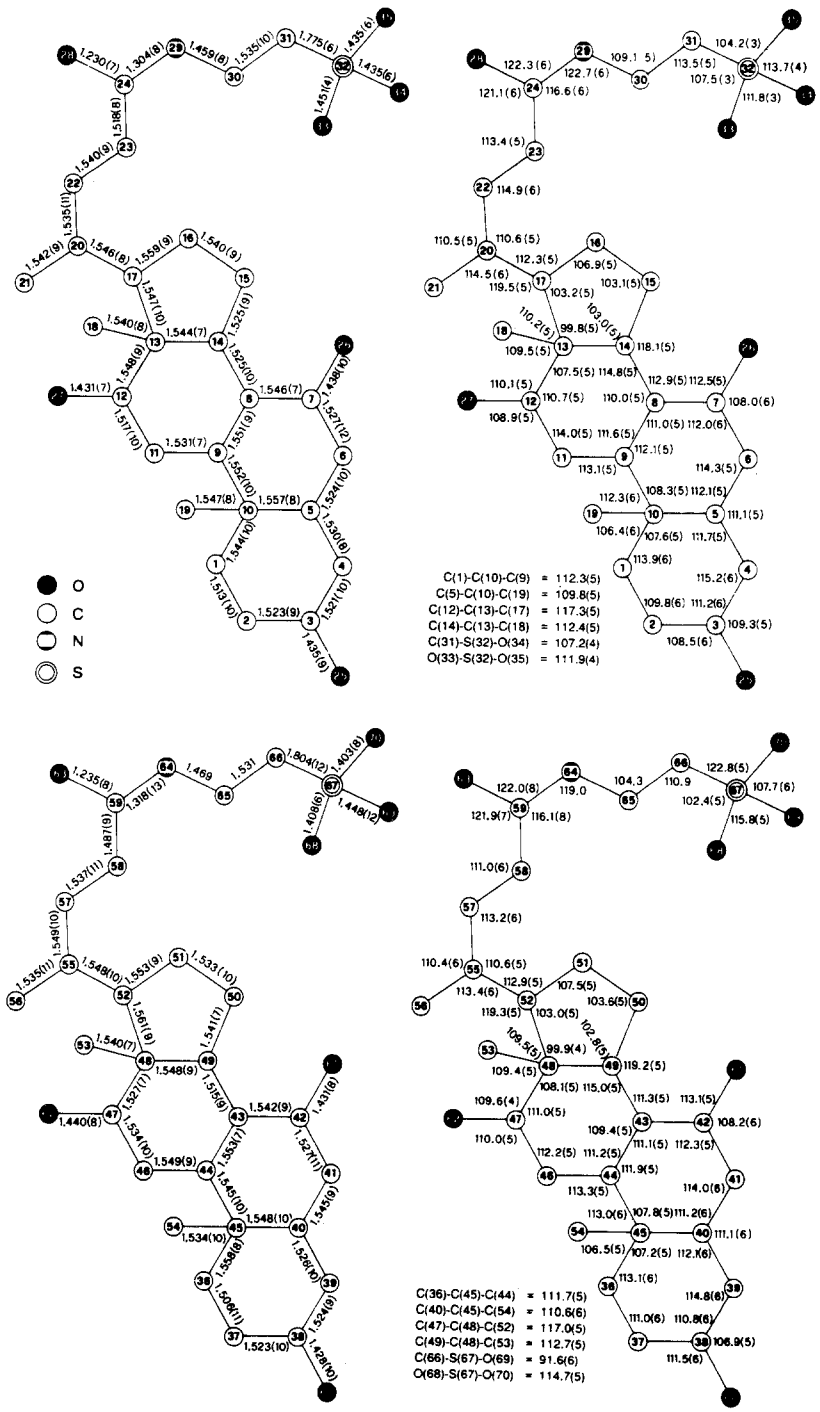

Fig. 1. Final bond distances (Å) and bond angles (°) found for the taurocholate anions. E.s.d.'s in parentheses.

Table I. Fractional atomic coordinates ($\times 10^4$) and equivalent isotropic thermal parameters ($\times 10^3$) together with e.s.d.s in parentheses.

Atom	x/a	y/b	z/c	U_{eq}(Å^2)*
Na(1)	12343(2)	6815(2)	7575(4)	52(1)
Na(2)	2994(2)	5819(2)	1932(4)	56(1)
C(1)	11688(5)	2549(5)	12732(8)	43(2)
C(2)	12332(5)	3477(5)	12477(8)	42(2)
C(3)	13038(5)	3780(5)	14248(9)	44(2)
C(4)	12343(5)	3626(4)	15722(8)	40(2)
C(5)	11614(5)	2710(4)	15928(8)	37(2)
C(6)	10910(6)	2635(5)	17370(8)	45(2)
C(7)	9961(6)	3077(5)	16832(7)	41(2)
C(8)	9264(5)	2814(4)	14993(7)	32(2)
C(9)	10011(5)	2925(4)	13557(7)	30(2)
C(10)	10902(5)	2403(4)	14108(8)	36(2)
C(11)	9326(5)	2740(4)	11696(7)	39(2)
C(12)	8451(5)	3245(4)	11131(7)	36(2)
C(13)	7661(4)	3072(4)	12513(7)	29(2)
C(14)	8374(5)	3307(4)	14353(7)	31(2)
C(15)	7514(5)	3240(4)	15538(7)	39(2)
C(16)	6621(6)	3613(4)	14289(8)	42(2)
C(17)	6872(5)	3671(4)	12352(7)	33(2)
C(18)	6999(5)	2121(4)	12518(8)	39(2)
C(19)	10388(7)	1419(4)	14286(11)	53(2)
C(20)	5809(5)	3520(4)	10925(8)	37(2)
C(21)	5995(6)	3443(4)	9018(8)	45(2)
C(22)	5193(5)	4221(5)	10922(8)	42(2)
C(23)	5777(6)	5128(4)	10221(8)	44(2)
C(24)	5463(5)	5299(4)	8213(8)	37(2)
O(25)	13540(4)	4686(3)	14013(7)	54(2)
O(26)	10422(4)	3993(4)	16873(7)	52(2)
O(27)	8984(4)	4145(3)	10972(6)	51(2)
O(28)	4489(4)	5162(3)	7482(6)	44(2)
N(29)	6276(4)	5606(3)	7323(7)	40(2)
C(30)	6102(5)	5876(4)	5419(8)	38(2)
C(31)	5883(6)	6778(4)	5185(8)	42(2)
S(32)	5746(1)	7210(1)	2928(2)	36(1)
O(33)	4790(4)	6648(3)	1919(6)	47(2)
O(34)	6746(4)	7230(4)	2304(8)	66(2)
O(35)	5578(6)	8049(3)	3024(7)	62(2)
C(36)	3389(6)	10100(5)	−5646(8)	44(3)
C(37)	2900(6)	9143(5)	−5742(8)	46(2)
C(38)	2048(5)	8817(5)	−4509(8)	46(2)
C(39)	2534(6)	9088(5)	−2612(9)	46(2)
C(40)	3101(6)	10046(5)	−2481(8)	43(2)
C(41)	3613(6)	10252(5)	−523(9)	49(3)
C(42)	4635(5)	9911(4)	208(7)	40(2)
C(43)	5485(5)	10150(4)	−1073(7)	32(2)
C(44)	4926(5)	9918(4)	−3012(7)	32(2)
C(45)	3974(5)	10361(4)	−3727(7)	38(2)
C(46)	5793(5)	10088(4)	−4267(7)	38(2)
C(47)	6712(5)	9622(4)	−3552(7)	36(2)
C(48)	7294(5)	9888(3)	−1681(7)	31(2)
C(49)	6411(5)	9700(3)	−453(7)	31(2)

Table I. (continued).

Atom	x/a	y/b	z/c	U_{eq}(Å^2)*
C(50)	7115(5)	9850(4)	1423(7)	37(2)
C(51)	8120(5)	9506(4)	1361(8)	39(2)
C(52)	8084(5)	9340(4)	−618(7)	34(2)
C(53)	7925(6)	10846(4)	−1791(9)	42(2)
C(54)	4362(7)	11349(5)	−3840(10)	52(3)
C(55)	9248(5)	9478(4)	−1097(9)	42(2)
C(56)	9223(7)	9302(6)	−3042(10)	61(3)
C(57)	9922(6)	8924(5)	214(10)	47(2)
C(58)	9480(6)	7951(5)	−21(8)	45(2)
C(59)	9796(5)	7440(5)	1657(9)	46(2)
O(60)	1694(5)	7897(4)	−4395(7)	60(2)
O(61)	4278(4)	9001(3)	615(6)	48(2)
O(62)	6256(4)	8702(3)	−3500(6)	42(2)
O(63)	10760(4)	7395(4)	2199(7)	55(2)
N(64)	8991(9)	7052(7)	2549(14)	88(2)[b]
C(65)	9141(0)[a]	6333(0)[a]	3862(0)[a]	109(4)[b]
C(66)	9129(10)	6663(8)	5660(15)	82(3)[b]
S(67)	9344(1)	5869(1)	7474(2)	45(1)
O(68)	10486(5)	6145(5)	8114(9)	75(3)
O(69)	8630(8)	6129(6)	8453(13)	105(2)[b]
O(70)	8949(7)	4978(5)	7291(11)	86(3)
O(1)	12545(4)	7249(3)	634(7)	53(2)
O(2)	2681(5)	5372(4)	8923(7)	55(2)
O(3)	11009(5)	5394(4)	11751(9)	68(2)
O(4)	4354(5)	7358(4)	−1913(7)	63(2)
O(5)	12289(10)	6202(8)	14794(17)	123(3)[b]

*$U_{eq} = 1/3\ \Sigma_i \Sigma_j U_{ij} a_i^* a_j^*\ \mathbf{a}_i \mathbf{a}_j$), where U_{ij} are thermal parameters, expressed as mean-square amplitudes of vibration, and $\mathbf{a}$ and a^* are unit cell direct axis and reciprocal axis moduli, respectively.

[a]These coordinates were kept fixed during the refinement.

[b]Isotropic temperature factor.

and bond angles are given. The structure factor list has been deposited as Supplementary Data.

3. Results and Discussion

3.1. MOLECULAR STRUCTURE

The bond distances and bond angles are in satisfactory agreement with those usually reported in the literature. However, those involving the side chain atoms, starting from N(64), of the second NaTC anion show less reliable values with greater standard deviations. No evidence of disorder was detected, so the less accurate location of these atoms, compared with that of the corresponding ones of the first NaTC anion, can be ascribed to their greater thermal motion.

Ring D approaches the half-chair conformation, especially in the case of the first anion, and is coupled with the *gauche* conformation of the C(17)—C(20)—C(22)—C(23) torsion angle, as is generally the case [17]. The cyclopentane torsion angles are given, according to the convention of Klyne and Prelog [18], in Table II, together with the pseudorotation phase angle Δ and the maximum torsion angle φ_m [19]. The side chain conformations of the two anions differ, beginning from the C(22)—C(23) torsion angle, which has remarkable conformational flexibility and is largely responsible for the side chains turning in two approximately opposite directions (see Figure 2). The values observed for these torsion angles (see Table II) do not correspond to potential energy minima [17]; therefore, the experimental conformations are controlled mainly by ion-ion interactions and intermolecular hydrogen bonds. Moreover, the deviation from planarity of the peptide group in the second anion (assuming that the three bonds to N(64) lie in a plane) is rather unusual: the torsion angle O(63)—C(59)—N(64)—C(65) is −20°. NaTDC (see Table II), NaGDC [6], and NaGC [11] give rise to different side chain conformations, too, confirming that the bile salts can assume several permissible conformations in order to satisfy packing requirements.

3.2. CRYSTAL PACKING

The NaTC crystal is formed of bilayers held together along *b* by weak van der Waals forces involving chiefly methyl groups (see Figure 3). The bilayers extend in

Table II. Torsion angles of the NaTC side chain and ring D together with Δ and φ_m(°). Estimated standard deviations in parentheses. The values for NaTDC are reported for comparison.

	NaTC first anion	NaTC second anion	NaTDC
C(13)—C(17)—C(20)—C(21)	−50.7(8)	−59.9(8)	−55.1(7)
C(13)—C(17)—C(20)—C(22)	−176.3(5)	175.5(5)	−177.1(5)
C(17)—C(20)—C(22)—C(23)	69.3(7)	69.3(7)	−161.7(5)
C(20)—C(22)—C(23)—C(24)	89.5(7)	−155.6(6)	68.1(8)
C(22)—C(23)—C(24)—O(28)	50.8(9)	−70.7(9)	65.2(8)
C(22)—C(23)—C(24)—N(29)	−130.1(6)	108.0(9)	−112.2(8)
C(23)—C(24)—N(29)—C(30)	−174.2(6)	160.9	165.6(8)
C(24)—N(29)—C(30)—C(31)	79.6(7)	115.5	−84.3(11)
O(28)—C(24)—N(29)—C(30)	5.0(10)	−20.4	−11.7(15)
N(29)—C(30)—C(31)—S(32)	176.2(4)	−178.4	−166.9(6)
C(30)—C(31)—S(32)—O(33)	62.6(5)	96.7	48.2(8)
C(30)—C(31)—S(32)—O(34)	−57.7(6)	−146.4	−72.5(8)
C(30)—C(31)—S(32)—O(35)	−178.5(5)	−34.0	167.8(7)
C(17)—C(13)—C(14)—C(15)	49.3(5)	48.2(5)	46.9(6)
C(13)—C(14)—C(15)—C(16)	−38.7(6)	−36.8(6)	−35.8(7)
C(14)—C(15)—C(16)—C(17)	13.1(6)	10.9(6)	9.9(8)
C(15)—C(16)—C(17)—C(13)	17.1(6)	18.7(6)	18.5(8)
C(16)—C(17)—C(13)—C(14)	−39.9(6)	−40.5(5)	−39.4(7)
Δ	3.9	9.0	9.7
φ_m	49.3	48.3	47.1

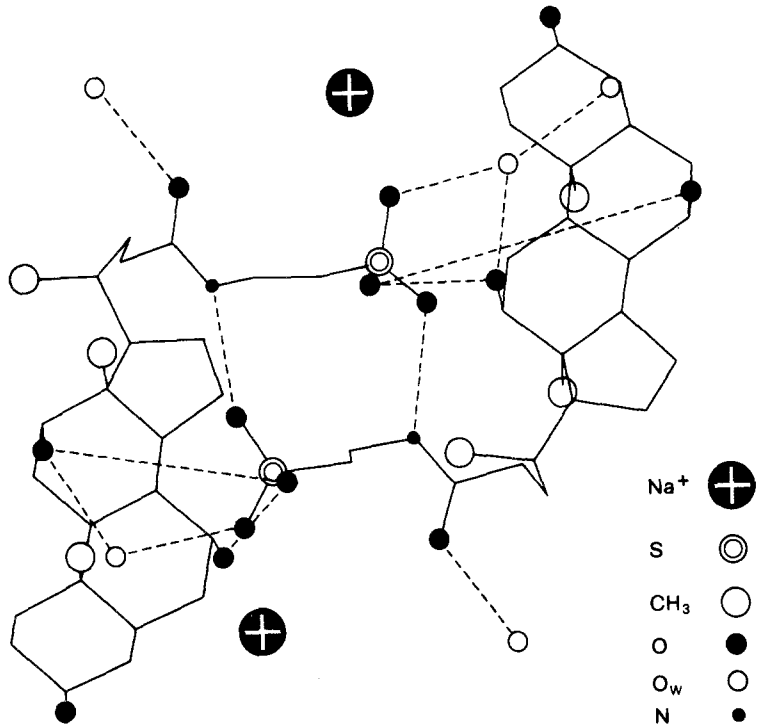

Fig. 2. View of the two NaTC anions of the asymmetric unit along the direction perpendicular to a^*c. Broken lines represent hydrogen bonds.

planes parallel to *ac*. Rows of NaTC molecules extend along *a*; the molecules in each row are linked by head-to-tail polar interactions. Translation of a row along *c* gives rise to a monolayer. Each bilayer is composed of two antiparallel monolayers, and is stabilized by strong ion–ion, ion–dipole, and hydrogen bonding forces. Sodium ions and water molecules fill small channels, whose inner surface consists of sulfonate, hydroxyl, and carboxyl groups. The sodium ions, hexa-coordinated as in NaTDC, show a distorted octahedral coordination (Figure 4). Each sodium ion is engaged in a Coulombic interaction with one O(33) and in ion-dipole interactions with one O(25) hydroxyl group and four water molecules. Three water oxygen atoms, namely O(1), O(2) and O(5), coordinate with both sodium ions. An extensive network of hydrogen bonds characterizes the bilayer (see Table III). The long distances between O(4) and O(33) and between O(4) and O(62) might raise some doubt about the formation of hydrogen bonds, in both of which O(4) behaves as donor atom, since O(62) is the donor atom in the hydrogen bond with O(35). However, the O(33)—O(4)—O(62) angle of $\sim 119°$ and the coordination of O(4) with $Na^+(1)$ alone in the absence of hydrogen bonding suggest that O(4) is indeed the donor in two weak hydrogen bonds.

The two anions of the asymmetric unit (see Figure 2) are held together and stabilized by several hydrogen bonds (see Table III). This unit is joined to adjacent ones mainly by strong polar interactions involving sodium ions, water molecules,

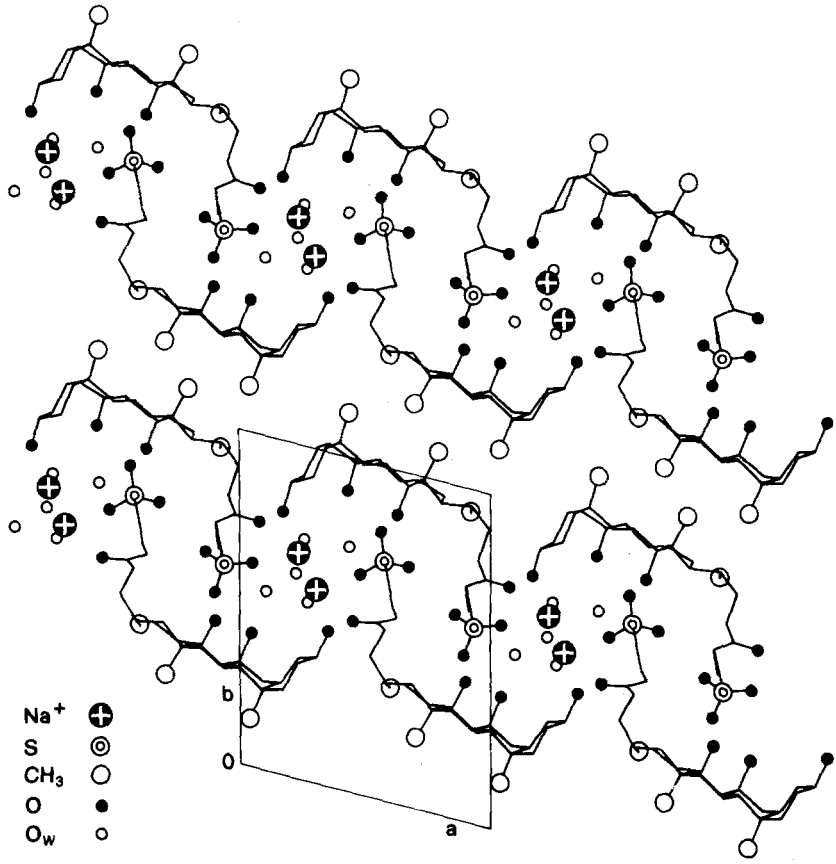

Fig. 3. Crystal packing of the NaTC crystal viewed along *c*.

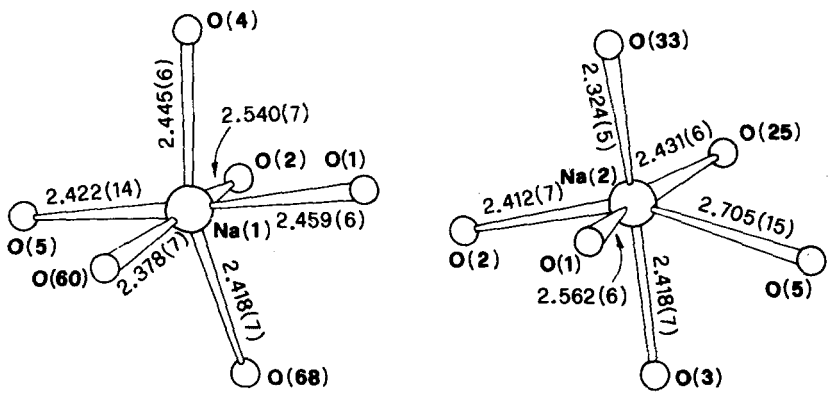

Fig. 4. Coordination of the sodium ions viewed along the direction perpendicular to a^*c. The Na^+—O distances (Å) are shown.

Table III. O—O distances (Å) in the hydrogen bonds. Estimated standard deviations are in parentheses.

O(25)—O(28)[a]	2.790(7)
O(26)—O(70)[b]	2.839(12)
O(27)—O(70)	2.967(9)
O(27)—O(3)	2.825(7)
O(28)—O(2)	2.846(9)
N(29)—O(69)	2.874(11)
O(33)—O(4)	3.016(7)
O(34)—N(64)	2.915(13)
O(35)—O(61)	2.825(8)
O(35)—O(62)[b]	2.855(7)
O(60)—O(63)[c]	2.755(7)
O(62)—O(4)	3.127(7)
O(63)—O(1)	2.837(8)
O(68)—O(3)	2.922(9)
O(3)—O(5)	2.800(13)

Symmetry code: (a) $x+1$, y, $z+1$; (b) x, y, $z+1$; (c) $x-1$, y, $z-1$.

sulfonate, hydroxyl, and carboxyl groups. The best growing direction is parallel to *c*, since the strongest interactions are generated around the axis of the channel filled with sodium ions and water molecules; the second best growing direction is parallel to *a*. Thus, one could identify as the most stable unit that visible in Figure 3 in projection, composed of the four molecules which partly lie within the unit cell and of those obtained by translation along *c*. Of course, the ratio between the sodium ions inside the bilayer and those at the edge of the bilayer is 1 and increases by welding of asymmetric units along *a*. Therefore, supposing that the bilayer adequately represents the NaTC micelle, the ratio between the sodium ions inside the micelle and those outside the micelle in contact with the solvent molecules increases when the bilayer grows along *a*.

It is noteworthy that sodium cholate [20] and rubidium deoxycholate [21] give rise to bilayers similar to that of NaTC, in crystals grown from organic solvents. Although in the case of RbDC the structure of the micellar aggregates in aqueous solution was proved to be helical [2, 3], and helices were found in the crystal obtained from water [12], there is some probability that the lamellar structural unit of NaTC previously described can exist in aqueous solution. In fact, for bile salt micelles with low aggregation numbers, as in the case of NaTC, the bilayer could be preferred to the helix, which generally needs several monomers in order to be stabilized. By contrast, micelles of NaTDC exhibit higher aggregation numbers and a helical structure [8, 10], as has been recently confirmed by small-angle X-ray scattering measurements (unpublished data of Giglio, Morpurgo, and Pavel).

Further work is in progress in order to study the other two crystalline phases of NaTC.

Acknowledgements

The authors wish to thank Prof. D. Braga (University of Bologna) for data collection. The Italian Ministero dell'Università e della Ricerca Scientifica e Tecnologica and the Italian Consiglio Nazionale delle Ricerche–Progetto Finalizzato Chimica Fine e Secondaria–are gratefully acknowledged for financial support.

References

1. G. Conte, R. Di Blasi, E. Giglio, A. Parretta, and N. V. Pavel: *J. Phys. Chem.* **88**, 5720 (1984).
2. G. Esposito, E. Giglio, N. V. Pavel, and A. Zanobi: *J. Phys. Chem.* **91**, 356 (1987).
3. E. Giglio, S. Loreti, and N. V. Pavel: *J. Phys. Chem.* **92**, 2858 (1988).
4. A. R. Campanelli, S. Candeloro De Sanctis, E. Giglio, N. V. Pavel, and C. Quagliata: *J. Incl. Phenom.* **7**, 391 (1989).
5. M. D'Alagni, M. L. Forcellese, and E. Giglio: *Colloid Polym. Sci.* **263**, 160 (1985).
6. A. R. Campanelli, S. Candeloro De Sanctis, E. Chiessi, M. D'Alagni, E. Giglio, and L. Scaramuzza: *J. Phys. Chem.* **93**, 1536 (1989).
7. G. Esposito, A. Zanobi, E. Giglio, N. V. Pavel, and I. D. Campbell: *J. Phys. Chem.* **91**, 83 (1987).
8. E. Chiessi, M. D'Alagni, G. Esposito, and E. Giglio: *J. Incl. Phenom.* **10**, 453 (1991).
9. M. C. Carey: in *Sterols and Bile Acids* (eds. H. Danielsson and J. Siovall), pp. 345–403, Elsevier/North-Holland Biomedical Press, Amsterdam (1985).
10. A. R. Campanelli, S. Candeloro De Sanctis, E. Giglio, and L. Scaramuzza: *J. Lipid Res.* **28**, 483 (1987).
11. A. R. Campanelli, S. Candeloro De Sanctis, L. Galantini, E. Giglio, and L. Scaramuzza: *J. Incl. Phenom.* **10**, 367 (1991).
12. A. R. Campanelli, S. Candeloro De Sanctis, E. Giglio, and S. Petriconi: *Acta Crystallogr.* Sect. **C40**, 631 (1984).
13. J. Lon Pope: *J. Lipid Res.* **8**, 146 (1967).
14. T. Debaerdemaeker, G. Germain, P. Main, L. S. Refaat, C. Tate, and M. M. Woolfson: *MULTAN 88.* Computer Programs for the Automatic Solution of Crystal Structures from X-ray Diffraction Data. University of York, England (1988).
15. D. J. Watkin and J. R. Carruthers: *CRYSTALS User Guide*, Chemical Crystallography Laboratory, University of Oxford, England (1981).
16. *International Tables for X-Ray Crystallography*, Vol. 4, J. A. Ibers and W. C. Hamilton, Kynoch Press, Birmingham, England, 1974, p. 99. (Distributed by Kluwer Academic Publishers Group, Dordrecht, the Netherlands.)
17. E. Giglio and C. Quagliata: *Acta Crystallogr.* **B31,** 743 (1975).
18. W. Klyne and V. Prelog: *Experientia* **16**, 521 (1960).
19. C. Altona, H. J. Geise, and C. Romers: *Tetrahedron* **24**, 13 (1968).
20. R. E. Cobbledick and F. W. B. Einstein: *Acta Crystallogr.* **B36**, 287 (1980).
21. V. M. Coiro, E. Giglio, S. Morosetti, and A. Palleschi: *Acta Crystallogr.* **B36**, 1478 (1980).